Factors affecting the photoelectrochemical fixation of carbon dioxide with semiconductor colloids

Brian R. Eggins[a,*], Peter K.J. Robertson[b], Eileen P. Murphy[a], Elaine Woods[a], John T.S. Irvine[c]

[a] *School of Biological and Chemical Sciences, University of Ulster at Jordanstown, Shore Road, Newtownabbey, Co. Antrim, BT37 0QB, Northern Ireland, UK*
[b] *School of Applied Sciences, The Robert Gordon University, St Andrew Street, Aberdeen, AB25 1HG, Scotland, UK*
[c] *Department of Chemistry, University of St. Andrews, College Gate, North Street, St. Andrews, KY16 9AJ, Scotland, UK*

Abstract

Carbon dioxide was reduced photocatalytically using aqueous CdS or ZnS colloids containing tetramethylammonium chloride to give the dimeric and tetrameric products namely, oxalate, glyoxylate, glycolate and tartrate. A model is presented to explain the role of the tetramethylammonium ions. Studies were also performed using ZnO, SiC, BaTiO$_3$ and Sr TiO$_3$, which in the absence of tetramethylammonium ions produced formate and formaldehyde. The relative quantum efficiencies of the six semiconductors were related to their band gaps and conduction band potentials. The role and effectiveness of several 'hole acceptor' (electron donor) compounds in this process is shown to be related to their redox potentials. © 1998 Elsevier Science S.A. All rights reserved.

1. Introduction

The electrochemical and photoelectrochemical reduction of carbon dioxide has been a topic of interest and sometimes controversy for many years [1]. Usually the formation of single carbon products such as formate or formaldehyde have been reported [1]. We have confirmed and developed the observations of Bewick [2,3] that the electrochemical reduction of carbon dioxide in aqueous solutions containing tetraalkylammonium salts results in the generation of dimeric and tetrameric products. These observations have been rationalised by ourselves [4] and Gressin [5] with the mechanisms shown in Figs. 1 and 2.

The addition of one electron to a carbon dioxide molecule produces a carbon dioxide radical anion, which has been detected by Aylmer-Kelly [6] and Lamy [7]. This radical may be protonated leading to formate; it may be disproportionate to carbon monoxide and carbonate or it may dimerise giving oxalate (Fig. 1). It is with this latter route that our work is concerned. Fig. 2 shows the range of products possible from further reduction of oxalate. Electrochemical

reduction of carbon dioxide under these conditions has been shown to lead to oxalate [8], glyoxylate [4,9], glycolate [2,10], tartrate [9] and malate [3].

Our analysis of the cyclic voltammetry of carbon dioxide in aqueous tetramethylammonium perchlorate has further developed the mechanism at the electrode surface [11].

Semiconductors are powerful photo-redox catalysts. A semiconductor particle can act as a microelectrochemical cell [12], which is activated by photolysis. The use of simple semiconductor particles to reduce carbon dioxide was first reported by Halmann et al. in 1978 [13–17]. The products they obtained were mainly formate, and occasionally formaldehyde and methanol. Henglein [17] continued these studies using mainly cadmium sulphide (CdS) or zinc sulphide (ZnS) particles. With the latter he claimed to obtain quantum yields for formate of up to $\phi=0.8$ using sulphite or propan-2-ol as hole acceptors.

In 1988 and 1990 we [18,19] showed that in the presence of tetramethylammonium chloride the formation of glyoxylic, acetic and oxalic acids occurred as well as the expected formate, formaldehyde and methanol when carbon dioxide was photolysed over cadmium sulphide. Similar results were then obtained with zinc sulphide with the additional formation of glycolic and tartaric acids [20].

*Corresponding author. Tel.: +44-1232-366113; fax: +44-1232-366812; e-mail: br.eggins@ulst.ac.uk

$$CO_2 \xrightarrow{+e^-} CO_2^- \nearrow CO + CO_3^{2-} \text{ (Disproportionation)}$$

$$CO_2^- \xrightarrow{H^+} HCO_2^- \xrightarrow{H^+} HCO_2H \text{ (Protonation)}$$

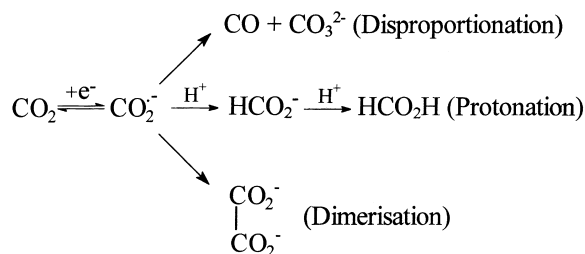$$\begin{array}{c} CO_2^- \\ | \\ CO_2^- \end{array} \text{ (Dimerisation)}$$

Fig. 1. One electron addition to carbon dioxide.

We have also reported the photocatalytic reduction of glyoxylic acid using the anthraquinone radical anion as photocatalyst and obtained tartaric, glycolic and malic acids [21].

The mechanistic steps involved in photocatalysis with semiconductor particles have been reported [19,22].

In this paper, we report and comment on the products formed and discuss the unexpected role of tetramethylammonium salts in facilitating the formation of dimeric and tetrameric products. We discuss the relative effectiveness of different semiconductors as photocatalysts in relation to their band-gap and conduction band semiconductors as photocatalysts in relation to their band-gap and conduction band potentials.

In all redox reactions, if there is a reduction, there must also be a corresponding oxidation. Consequently we have examined the role of 'hole acceptors' which assist on completing the oxidation part of the process. Their effectiveness is shown to be related to their redox potentials. Finally, we consider some processes which limit the effectiveness of semiconductor photocatalysis.

2. Experimental

2.1. Materials

Cadmium sulphide (99.99%, Koch Light), strontium titanate (98%, Goodfellow), barium titanate (99%, Bentron), zinc oxide (99.99%, Koch Light) and silicon carbide (carborundum, extra fine, BDH) were used as received.

Colloidal cadmium (or zinc) sulphide was prepared by the addition of sodium sulphide (BDH) (5 cm^3, 10^{-2} M) to cadmium chloride (or zinc sulphate) (5 cm^3, 10^{-2} M) in water (90 cm^3) while stirring. The solution was then diluted to produce solutions of 10^{-2} and 5×10^{-2} M of the appropriate sulphide.

Cadmium sulphide was doped with ruthenium oxide in the solid state using the method of Rajh and Micic [23]. Tetramethylammonium chloride (Aldrich) was used as supplied. The carbon dioxide (British Oxygen) was passed through a vanadium (II)/HCl solution to remove traces of oxygen. Deionised water was used in all experiments.

2.2. Photolysis

The appropriate electrolyte and other additives were mixed. The carbon dioxide was bubbled continuously through the solution which was then irradiated with light (320–580 nm) from a Phillips medium pressure mercury lamp of intensity 2.5×10^{-3} einsteins h^{-1} (determined by ferrioxalate actinometry [24]) for periods of 24–120 h.

2.3. Analysis

Samples of the solution were passed through a cation exchange column to remove the tetramethylammonium salts and then analysed for organic acids by HPLC using an Altex Isocratic Liquid Chromatograph with an Aminex HPX-87H ion exclusion column eluting with 0.016 M sulphuric acid. Detection of the acids was achieved using a Pye Unicam PU 4020 variable wavelength UV detector set at 210 nm. This technique was adopted for the detection of acetic, formic, glyoxylic, glycolic, tartaric, malic and oxalic acids [10].

Head space gas chromatography was adopted for the analysis of formaldehyde, methanol and acetaldehyde. A Perkin Elmer Sigma 3 Gas Chromatograph as used with a head space oven set at 60°C. The separations were performed on a 20 m Carbowax capillary column at 40°C using a nitrogen carrier gas at 8 psi and flame ionisation detection.

Glyoxylic acid was further identified by the violet colour reaction of phenylhydrazine/ferricyanide which was monitored at 540 nm [24,25]. Formaldehyde was estimated using
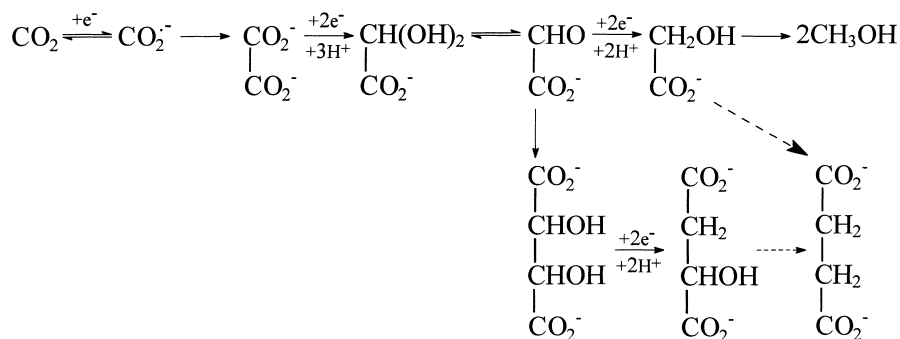
$$CO_2 \xrightarrow{+e^-} CO_2^- \longrightarrow \begin{array}{c} CO_2^- \\ | \\ CO_2^- \end{array} \xrightarrow[+3H^+]{+2e^-} \begin{array}{c} CH(OH)_2 \\ | \\ CO_2^- \end{array} \rightleftharpoons \begin{array}{c} CHO \\ | \\ CO_2^- \end{array} \xrightarrow[+2H^+]{+2e^-} \begin{array}{c} CH_2OH \\ | \\ CO_2^- \end{array} \longrightarrow 2CH_3OH$$

$$\begin{array}{c} CO_2^- \\ | \\ CHOH \\ | \\ CHOH \\ | \\ CO_2^- \end{array} \xrightarrow[+2H^+]{+2e^-} \begin{array}{c} CO_2^- \\ | \\ CH_2 \\ | \\ CHOH \\ | \\ CO_2^- \end{array} \dashrightarrow \begin{array}{c} CO_2^- \\ | \\ CH_2 \\ | \\ CH_2 \\ | \\ CO_2^- \end{array}$$

Fig. 2. Overall electrochemical reduction of carbon dioxide.

the Hantzsch reagent (acetylacetone in ammonium acetate/ acetic acid) monitored at 412 nm [25,26]. Colorimetric methods were also used to detect glyoxal, carbon monoxide, formate and acetaldehyde. The concentration of carbon dioxide was determined by titration with barium hydroxide solution.

3. Results

Table 1 displays the various products obtained on photolysis of ZnS suspensions in the presence of carbon dioxide at various pH values [20]. In addition to the single carbon products formate, formaldehyde and methanol generally reported we have also detected the dimerc products oxalate, glyoxylate, glycolate and tartrate.

The results obtained for the reduction of CO_2 on CdS are shown in Table 2. When TMACl was added to the electrolyte glyoxylate was detected which was not observed in the experiments which were carried out in the absence of this ion.

Blank runs performed in nitrogen rather than CO_2 for both photocatalysts resulted in no detectable products being generated.

The quantum yields for the reduction of carbon dioxide on different semiconductors are displayed in Table 3. In these experiments no tetraalkylammonium salts or electron donor compounds were added to the system. From the table it can be seen that the semiconductors with the most negative conduction band potentials provided the best yields, particularly CdS, SiC and ZnS.

CdS and ZnS can be readily prepared in the quantum crystallite, colloidal state with particle sizes around 2–4 nm [27–29]. Kanemoto et al. [29], Henglein et al. [17] have

Table 3
Comparison of different semiconductors

Semiconductor	E_{BG} (eV)	$V_{CB}(V)$ versus SHE	$\phi_{e'}$ (10^{-5})
SrTiO$_3$	3.2	−0.8	0.74
BaTiO$_3$	3.2	−0.4	2.1
CdS	2.5	−0.9	3.8
ZnO	3.2	−0.5	4.3
SiC	3.0	−1.4	6.7
ZnS	3.85	−2.0	[5400][a]

Suspensions of 0.3 g of each semiconductor in water (100 cm^3) at pH 4 saturated with CO_2 irradiated with 2.5×10^{-3} einsteins h^{-1} for 24 h ($250 < \lambda < 580$ nm). No TMACl or electron donors added. ϕ_e, was measured from yields of formic acid and formaldehyde.
[a] From work with ZnS ([29]), not strictly comparable.

shown that in these particles and their loose aggregates the band gap is increased and the rate of recombination of holes and electrons are decreased. There appears to be a useful correlation between the spectroscopic behaviour of semiconductors and the particle size and hence the band gap. Fig. 3 displays the absorption spectrum of our sample of colloidal zinc sulphide which when compared with Kanemoto's spectra [29] indicates that our sample is quantum crystallite.

The fact that the semiconductors with the most negative conduction band potential provided the best quantum yields is not surprising since these materials would have a stronger reducing potential.

Fig. 4 shows the formation of the dimeric product oxalate on ZnS versus reaction time. The effect of tetramethylammonium chloride is very dramatic; in its absence the yield of oxalate is close to the detection limit of $<10^{-7}$ mol dm^{-3}. The effect of sulphite as a hole acceptor also enhanced the yield but to a lesser extent.

Table 1
Yields of products generated by photocatalytic reduction of CO_2 on ZnS

pH	Irradiation time (h)	Oxalate (μmol dm^{-3})	Glyoxylate (μmol dm^{-3})	Glycolate (μmol dm^{-3})	Tartrate (μmol dm^{-3})	Formate (μmol dm^{-3})
2	36	900	1.9	–	–	–
4	24	1400	2.1	13	16	2.3
6	36	4	0.63	–	–	320
7	48	400	3.5	3.8	6.7	180
10	60	–	2.7	0.59	4.1	–
14	48	2300	–	–	–	–

Table 2
Yields of products generated by photocatalytic reduction of CO_2 on CdS

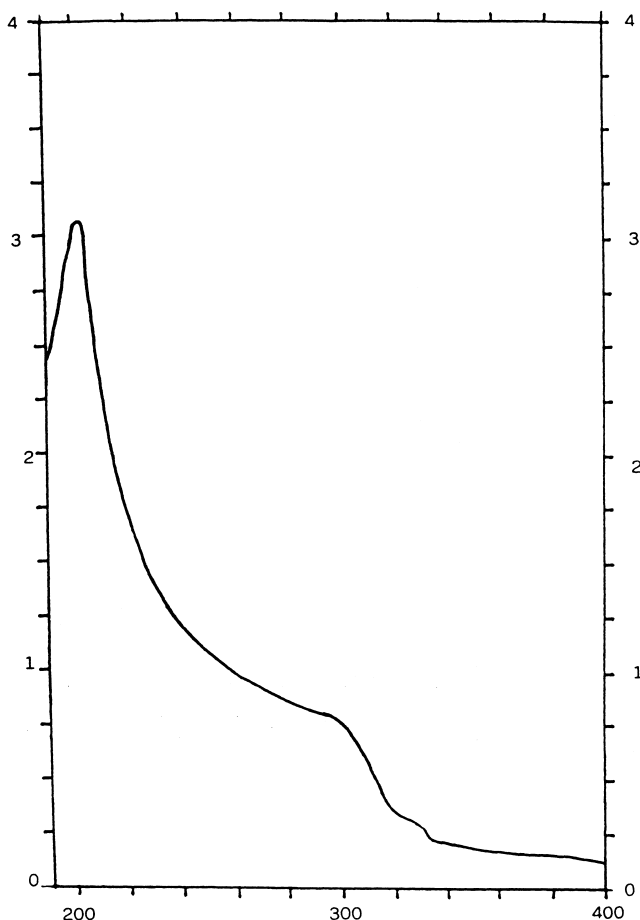| Solution	pH	Irradiation time (h)	Glyoxylate (μmol dm^{-3})	Acetate (μmol dm^{-3})	Formate (μmol dm^{-3})	Formaldehyde (μmol dm^{-3})	Methanol (μmol dm^{-3})
H$_2$O	4	94	–	3.5	75	11	87
TMACl	4	42	53	40	27	7	–
TMACl	6	42	66	–	136	6.1	–
TMACl	6	64	10.7	–	37	5.5	–

Fig. 3. Absorption spectrum of colloidal ZnS.

The use of alternative hole acceptors was examined using CdS as the photocatalyst for CO_2 reduction. CdS was chosen for this investigation since it has the smallest band gap and its conduction and valence band edge potentials overlap the redox range of the CO_2/HCO_2H reduction and H_2O/O_2 oxidation potentials, respectively (Fig. 5). The hole acceptor materials investigated are listed in Table 4 together with

Table 4
Comparison of different hole acceptors (electron donors)

Hole acceptor	$E°$(V) versus NHE	$e'(10^{-5})$	$6+\log e'$
None	–	0.53	0.72
Iodide	−0.54	0.96	0.98
TSCoPc	−0.66	1.7	1.23
$Fe(CN)_6^{3-}$	−0.69	1.6	1.20
Hydroquinone	−0.70	9.4	1.97
Sulphite	−0.95	103	3.01
Propan-2-ol	ca.−1.28	510	3.17
RuO_2	−1.3	0.94	0.97
Hypophosphite	−1.5	3500	4.54[a]

Suspensions of 0.3 g of CdS in water (100 cm^3) at pH 4 saturated with CO_2 irradiated with 3.9×10^{-3} einsteins h^{-1} for 24 h (250<λ<580 nm). No TMACl added. ϕ_e, was measured from yields of formic acid and formaldehyde.

[a] From work with ZnS [29].

their redox potential and corresponding quantum yields for the formation of formate and formaldehyde. A progressive improvement in quantum yield was observed with increasing redox potential of hole acceptor which is illustrated in Fig. 6.

An investigation was also carried out using ZnS as a photocatalyst and sulphite as a hole acceptor. The band edge potentials of ZnS also overlap the CO_2 reduction and water oxidation potentials, but the total band gap is much larger. The formation of glyoxylate and formaldehyde are shown in Fig. 7. With both products the positive effect of sulphite is very clear on a linear scale. At longer times these compounds are either reduced further or could be re-oxidised by the holes as has been observed by several other workers [19,30,31].

4. Discussion

The reduction of CO_2 using ZnS and CdS photocatalysts resulted in the detection of single carbon, dimeric and tetrameric products. The formation of the dihydroxy acid tartaric acid, is particularly interesting in that it parallels the natural photosynthetic process in which polyhydroxy compounds (sugars) are produced from carbon dioxide by a biological photocatalytic process. The formation of glycolic acid is also interesting since this together with tartaric acid has not been detected previously with photocatalytic reduction of CO_2. Surprisingly, only very small traces of oxalate were detected in the CdS system (less than 10^{-6} mol dm^{-3}). From Fig. 2 it can be seen that oxalate is an intermediate in the production of glyoxylate. The photolysis of oxalate solutions on CdS resulted in the production of glyoxylate, some tartrate, formate and carbon dioxide.

Some authors have raised the question as to whether these carbon compounds actually originated from carbon dioxide rather than from a breakdown product of, for example, the tetramethylammonium salts [32]. Experiments have been performed using ^{13}C labelled CO_2 in order to clarify this point [27,28]. In several cases it was shown that carbon monoxide from carbon dioxide reduction catalysed by ruthenium tripyridyl complexes was similarly labelled with ^{13}C. Hardly any carbon monoxide was detected in our experiments. Blank experiments performed in the absence of carbon dioxide gave no detectable carbon products. This would seem to be the indirect confirmation that the carbon products did originate from the carbon dioxide. Also, in experiments in which there was no added tetramethylammonium salt, the carbon dioxide was the only source of carbon for product formation. In these experiments the only products formed were formate or formaldehyde and sometime traces of methanol and acetaldehyde.

Caraway [33] has reported the photocatalytic oxidation of acetic acid using TiO_2. He obtained successively, glycolic acid and the glyoxylic acid, the reverse of our process. He also photo-oxidised glyoxylate to formate and subsequently
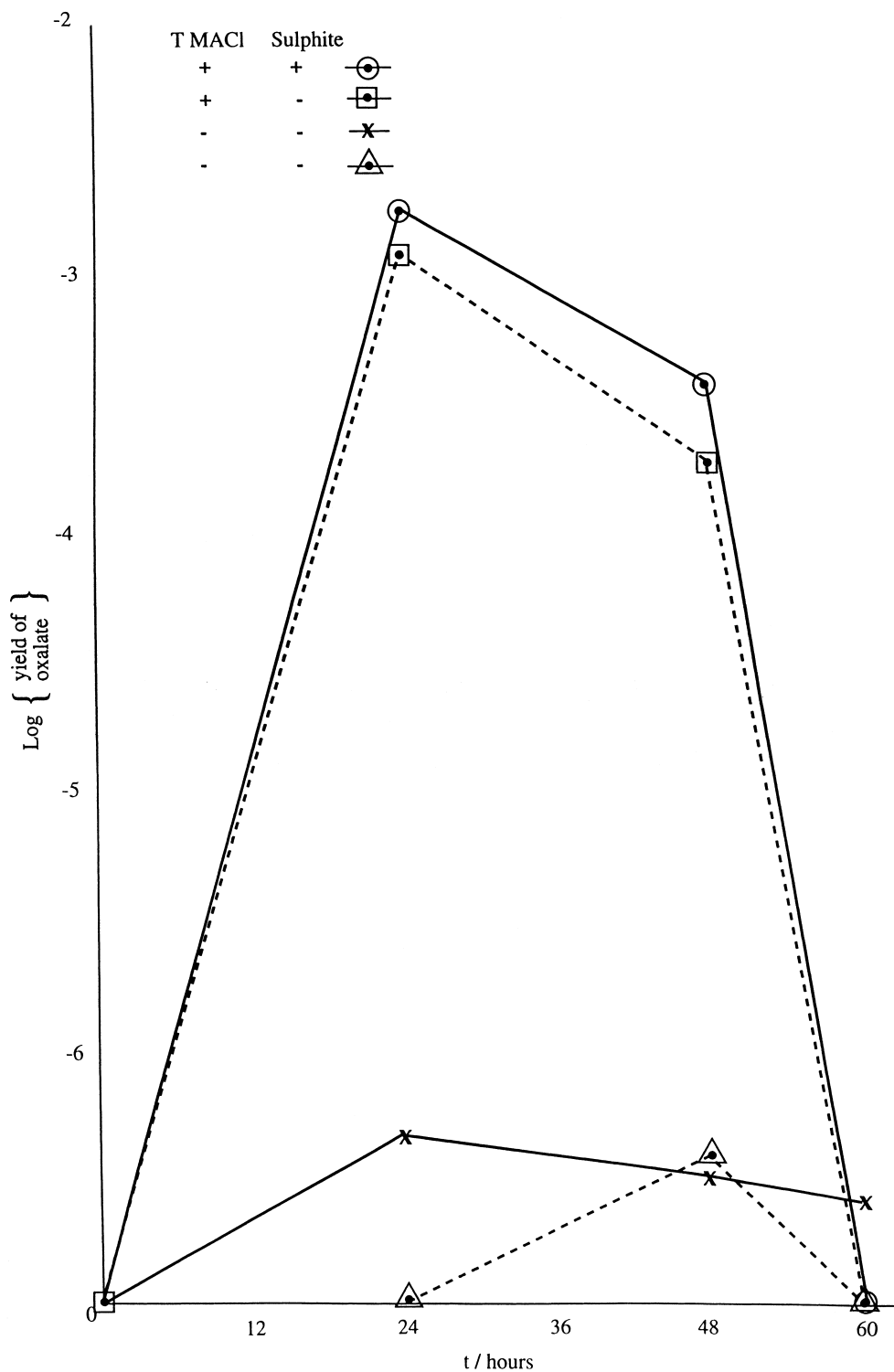
Fig. 4. Graph of oxalate yields against time on ZnS in the presence and absence of TMACl and sulphite.

CO_2. The quantum yields for our investigation would initially appear rather disappointing when compared to those obtained by other researchers [17,29]. This is due to the fact that different methods are used for calculating quantum yields by different workers [34]. The photonic efficiency (PE) of a photochemical process represents Eq. (1).

$$PE = \frac{\text{rate of reaction}}{\text{monochromatic light intensity}} \qquad (1)$$

The formal quantum efficiency (FQE) is calculated using Eq. (2).

$$FQE = \frac{\text{rate of reaction}}{\text{total light intensity}} \qquad (2)$$
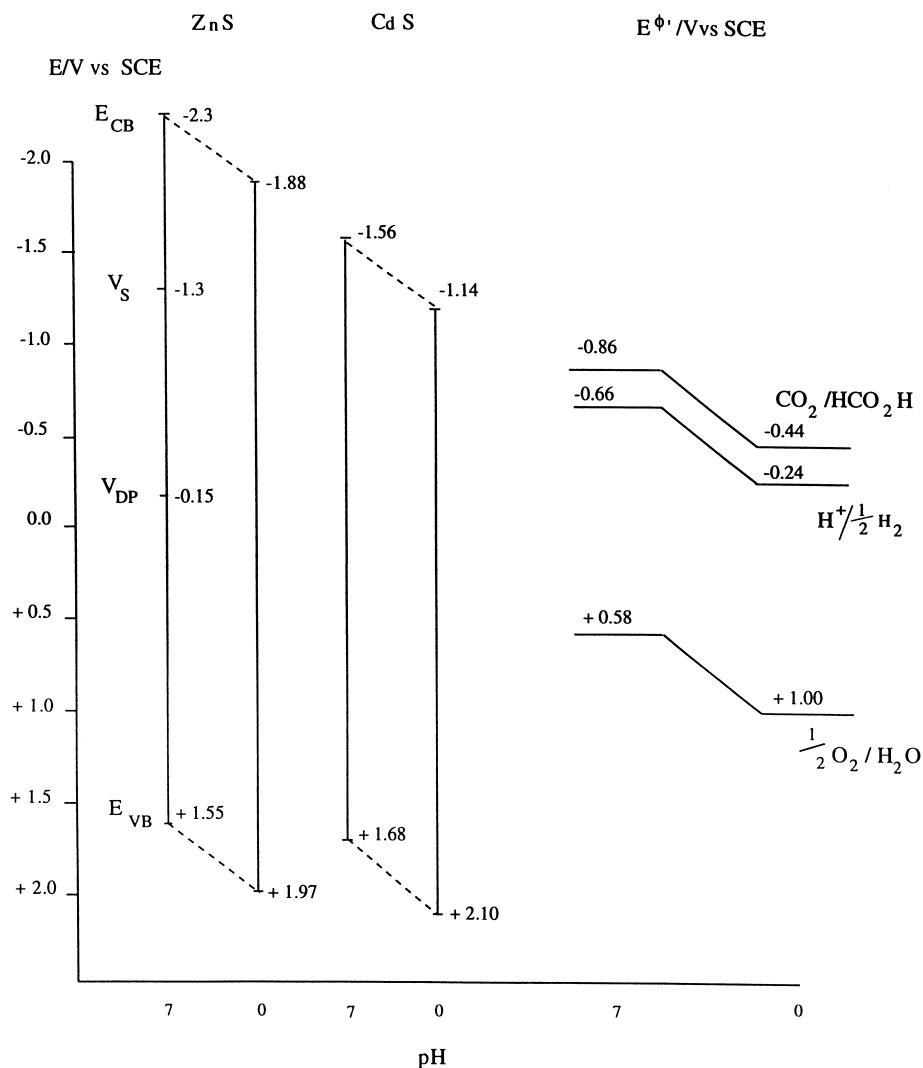
Fig. 5. Potential energy diagram for CdS and ZnS compared with electrode potentials of relevant reactions.

If monochromatic light is used FQE=PE otherwise FQE<PE. The values for FQE are usually significantly less than one. Semiconductor photocatalysis is influenced by a wide variety of parameters including the cell geometry, the structure and properties of the catalyst, intensity of illuminating radiation, pH and mass transport within the system. Comparing quantum efficiencies obtained by different groups for similar systems is difficult although the quantum efficiency does provide an indication of the overall efficiency of the photocatalytic process [34].

Kanemoto [29] used monochromatic light of wavelength 313 nm. The intensity was measured by ferrioxalate actinometry, and the yields were calculated assuming that two photons produced 1 mol of formate (or hydrogen). This gave relatively high quantum yields of ϕ=0.48, which represent the photonic efficiency. In all our work, however, we used broad-spectrum light and calculated the photon to electron conversion efficiency ϕ'_e. This quantity is not a true photochemical yield: it was calculated from the total incident

radiation intensity, rather than the number of photons absorbed by the semiconductor [19]. Thus our data in Table 3 are not directly comparable with quantum yields quoted by Henglein [17] and Kanemoto [29] since our values represent the formal quantum efficiency rather than photonic efficiency.

Our results indicate that the addition of tetraalkylammonium salts to the electrolyte does indeed promote the formation of dimeric and tetrameric products. The potential effect of these ions in the generation of dimeric products is illustrated in Fig. 8. This shows a schematic arrangement of ions and molecules in the vicinity of a semiconductor particle showing their correct relative sizes. There is a double layer of tetramethylammonium ions on the surface and halide ions position themselves further out. Three effects may be operating:

1. The large soft, positive tetraalkylammonium ions are adsorbed on the surface forming an almost aprotic layer excluding water [13].
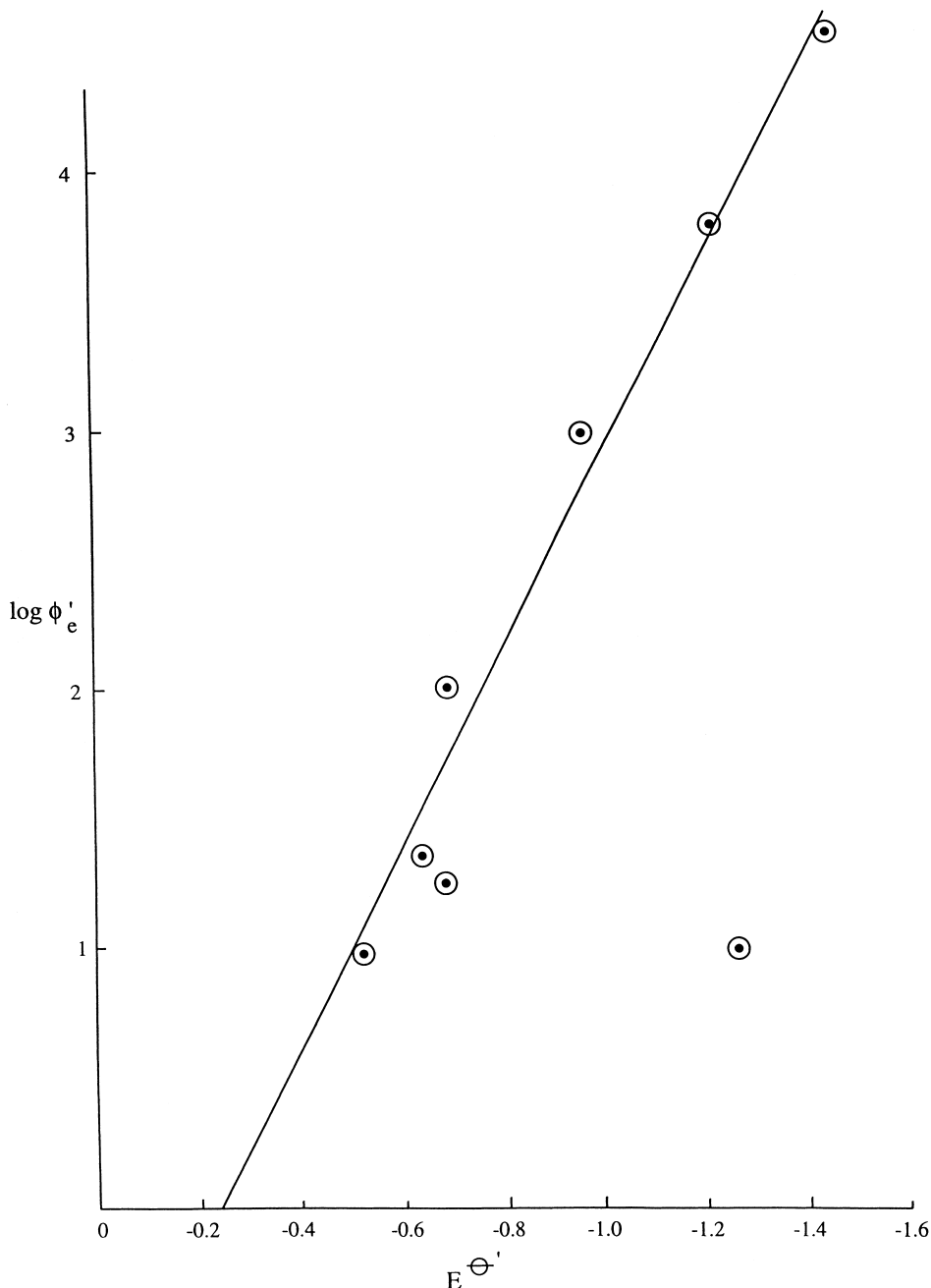
Fig. 6. Quantum yields of formate/formaldehyde on CdS versus redox potentials of various hole acceptors.

2. Unlike alkali metal ions (especially lithium), which are Lewis acids and encourage proton donation, tetraalkyl-ammonium ions have very low charge densities and hence a negligible Lewis acid effect [35].

3. The CO_2 molecules, and probably CO_2^- radical anions, are adsorbed at the particle surface [7,13–15] resulting in a high concentration of both species thus facilitating dimerisation by the Saveant mechanism [7,36] to oxalate.

The low proton availability at the surface permits the CO_2 radical anions to react with CO_2 molecules, followed by the

addition of an electron, to form oxalate (Fig. 1). The system is not strictly aprotic, so some protonation will occur allowing the formation of some formate. The oxalate can be protonated, permitting further reduction to glyoxylate, glycolate, tartrate and occasionally malate, which are observed on electrochemical reduction of CO_2 [2,3,10,11].

In the photocatalytic process the corresponding valence band oxidation process is often the formation of oxygen from water or alternatively photocorrosion of the semiconductor may occur. The addition of alternative 'hole acceptors' for which the reactions are more thermodynamically favourable than water decomposition can frequently
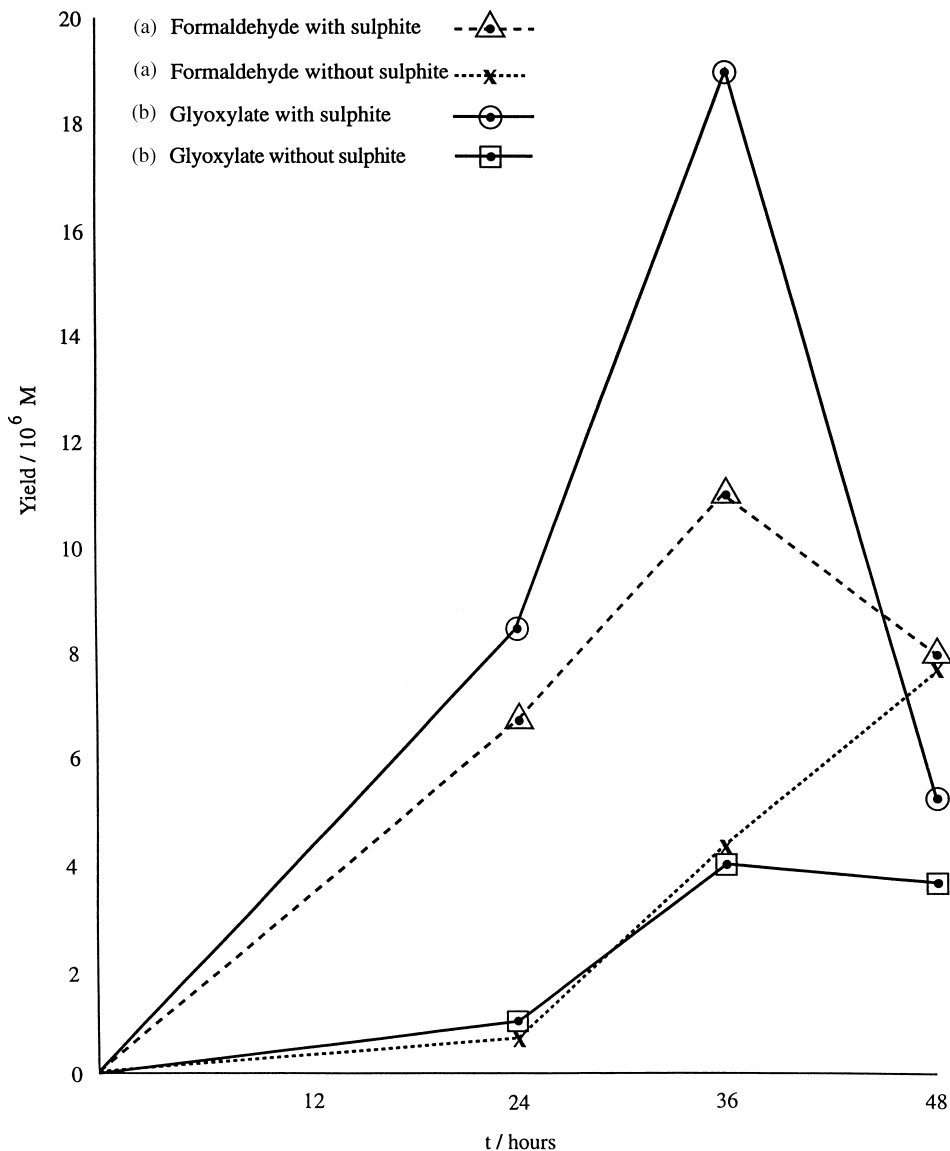
Fig. 7. Graph of product yields against time (a) formaldehyde; (b) glyoxylate; on ZnS in the presence and absence of sulphite.

improve quantum yields for photocatalytic reduction processes. An alternative method for enhancing the photocatalytic process is the addition of materials which catalyse water oxidation. The donation of electrons to the valence band hole may not be the only function of these hole acceptors which is shown by the marked deviations of the data for RuO_2, TSCoPC and $Fe(CN)_6^{3-}$. RuO_2 acts as a catalyst for water oxidation and resulted in a three-fold increase in yield of formate. This was not in proportion to the redox potential of RuO_2. Similarly TSCoPC was observed not to act as a sacrificial electron donor [37]. It may act as an oxidation catalyst, an electron relay or a sensitiser for the semiconductors [38]. Deviations with iodide and hexacyanoferrate (III), which were intended to be the sacrificial electron donors, are probably due to

experimental errors. The data for propan-2-ol was taken from Henglein's work [17]. The data for hypophosphite is from Kanemoto's work [29] on ZnS and is not strictly comparable, though it does fit in with the trends.

Several factors appear to limit the overall efficiency of the reduction of CO_2 using semiconductor photocatalysts. The activity of quantised ZnS colloids or suspensions requires a low density of surface defects such as sulphur vacancies and the presence of effective electron donors (hole acceptors). Kanemoto [29] used an electron donor which has an even higher electrode potential, hypophosphite, $H_2PO_2^-$. The mode of action is probably the one that is illustrated in the reactions given below.
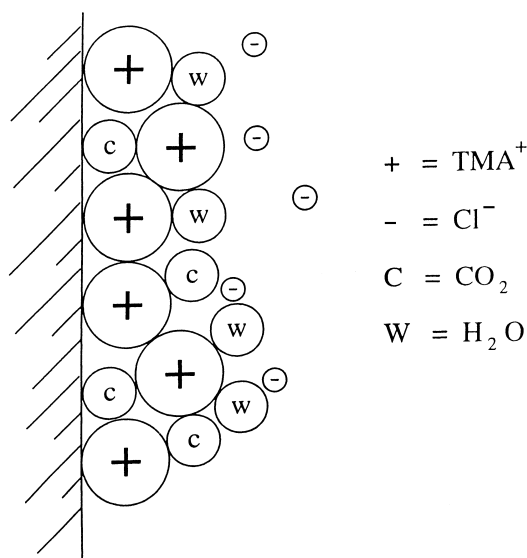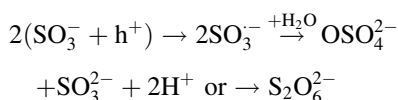
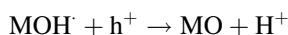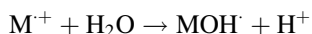$$H_2PO_2^- + 2H^+ + H_2O \rightarrow HPO_3^{2-} + 3H^+$$
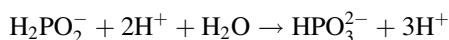
Fig. 8. Schematic diagram of adsorbed ions at the surface of a semiconductor particle.

$+$ = TMA$^+$

$-$ = Cl$^-$

C = CO$_2$

W = H$_2$O

Mechanisms suggested by Henglein [17] for the involvement of sulphite are a one hole disproportionation or a dimerisation mechanism (see the reaction given below).

$$2(SO_3^- + h^+) \rightarrow 2SO_3^- \overset{+H_2O}{\rightarrow} OSO_4^{2-}$$

$$+SO_3^{2-} + 2H^+ \text{ or } \rightarrow S_2O_6^{2-}$$

Other factors which limit overall efficiency are photocorrosion and electron trapping in vacancies. Metal chalcedonides are very prone to photocorrosion [19,38–41], that is, breakdown of the semiconductor itself. Often a brown discolouration of the catalyst is observed. The mechanisms shown in the reactions given below are general for photocorrosion processes.

$$MS + O \rightarrow MO + S$$

$$MS + h^+ \rightarrow M^{\cdot+} + S$$

$$M^{\cdot+} + H_2O \rightarrow MOH^{\cdot} + H^+$$

$$MOH^{\cdot} + h^+ \rightarrow MO + H^+$$

$$M = Cd \text{ or } Zn$$
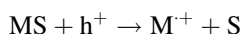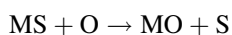
This process liberates protons and hence would be accelerated in solutions of higher pH.

In more acidic pH's hydrolysis will occur (see the reaction given below)

$$MS + H_2O \rightarrow MO + H_2S$$
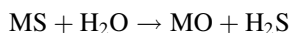
Another effect may occur in the presence of poor electron donors [29]. Lattice sulphide ions (S_2^-) may be converted to S_2^{2-} ions by anodic photocorrosion. This can occur above the anodic decomposition potential (ADP), reported to be -0.15 V versus SCE [29]. These lattice defects become hole trapping sites which oxidise electron donors. All these defects limit the suitability of metal chalcedonides as photocatalysts.

As normally produced, even quantum crystallites contain surface defects in the form of anion vacancies. These have been observed by Henglein [17] and Kanemoto [29] using fluorescence spectroscopy resulting in a band at $\lambda=420$ nm. Conductance band electrons can be trapped by these vacancies. Their energy level is about -1.3 V versus SCE, compared with the conduction band potential of -2.3 V versus SCE. This is insufficient to reduce carbon dioxide ($E^\circ < -2.21$ V versus SCE) but can still reduce hydrogen ions (water) ($E^\circ = -1.65$ V versus SCE). In many of their reactions Kanemoto et al. [29] found hydrogen as a major product as would be expected. The addition of sulphide, however, quenched the fluorescence at $\lambda=420$ nm, which they suggest is due to the elimination of surface vacancies. Now reduction of CO$_2$ could occur in competition with hydrogen formation. The quantum yield of hydrogen was 0.73 in the absence of CO$_2$. In the presence of CO$_2$ the quantum yields of H$_2$ and formate production were 0.48 and 0.24, respectively showing the level of competitive reduction.

We did not attempt to measure hydrogen evolution, nor did we add sulphide to minimise vacancies. Because of the presence of the tetraalkylammonium salts, resulting in a low proton availability at the particle surface, we did not consider hydrogen evolution likely. The presence of electron traps in the vacancies, however was most probable which could have been an important factor in reducing the yields of organic products. Henglein [41] suggested that low efficiencies are to be expected if the overall redox process involves both of the two electrons and two holes as with CO$_2$/formate or CdS/CdO. However with a one-electron/two-hole or a two-electron/one-hole process high quantum efficiencies may be obtained. CO$_2$/CO$_2^-$ is a one-electron process (though subsequent reduction of oxalate to glyoxylate is via two electrons).

5. Conclusions

A layer of relatively large tetraalkylammonium ions is adsorbed on the surface of the semiconductor particles forming an effectively aprotic layer, permitting the dimerisation of CO$_2$ radical anions to form oxalate. Since there are water molecules in the vicinity, oxalate can be reduced further to glyoxylate and thence to glycolate or tartrate, in an analogous manner to that established for the electrochemical reduction [11].

While the effectiveness of different semiconductors in reducing CO$_2$ is roughly in line with the order of increasing conduction band potentials, the variations, which are fairly small, may also be related to differences in particle size, which in quantum crystallites results in an increase in band gap and reduction in the rate of recombination of holes and electrons. Overall we observed quantum yields in the order: ZnS>SiC>ZnO>CdS>BaTiO$_3$>SrTiO$_3$.

The importance of hole acceptors has been emphasised. Following studies with I$^-$, TSCoPC, Fe(CN)$_6^{3-}$, hydroqui-

none, sulphite, propan-2-ol and hypophosphite, it was observed that the log of the quantum yield for most of them is in a linear relationship with their redox potentials. The main exception was RuO_2 which was operated by catalysing water oxidation rather than hole reduction.

References

[1] B.P. Sullivan, K. Krist, H.E. Guard (Eds.), Electrochemical and Electrocatalytic Reactions of Carbon Dioxide, Elsevier, Amsterdam, The Netherlands, 1993.

[2] A. Bewick, E.P. Greener, Tetrahedon Lett. (1969) 4623.

[3] A. Bewick, E.P. Greener, Tetrahedon Lett. (1970), 391.

[4] E.M. Bennett, B.R. Eggins, J. McNeill, E.A. McMullan, Anal. Proc. (1980) 356.

[5] J.C. Gressin, D. Michelet, L. Nadjo, J.-M. Saveant, Nouv. J. Chem. 3 (1979) 545.

[6] A.W. Aylmer-Kelly, A. Bewick, P.R. Cantrill, A.M. Tuxford, Faraday Disc. Chem. Soc. 56 (1974) 96.

[7] E. Lamy, L. Nadjo, J.-M. Saveant, J. Electroanal. Chem. 78 (1977) 403.

[8] D.A. Tysee, J.H. Wagenknecht, M.M. Baizer, J.L. Chruma, Tetrahedon Lett. (1972) 4809.

[9] B.R. Eggins, E.M. Graham, E.A. O'Neill, J. Grimshaw, Tetrahedon Lett. 29 (1972) 4809.

[10] B.R. Eggins, C. Ennis, R. McConnell, M. Spence, J. Appl. Electrochem. 27 (1997) 706.

[11] B.R. Eggins, E.M. Bennett, E.A. Bennett, E.A. McMullan, J. Electroanal. Chem. 408 (1996) 165.

[12] M.D. Archer, Chem. Br. 20 (1984) 991.

[13] M. Halmann, Nature 275 (1978) 115.

[14] B. Aurian-Blajeni, M. Halmann, J. Manassen, Solar Energy Mater. 8 (1983) 425.

[15] M. Ulman, A.H.A. Tinnemans, A. Mackor, B. Aurian-Blajeni, M. Halmann, Int. J. Solar Energy 1 (1982) 213.

[16] A.H.A. Tinnemans, T.P.M. Koster, D.H.M.W. Thewissen, A. Mackor, Solar Energy R&D Eur. Community Ser. D. Photochem. Photoelectrochem. and Photobiol. Proc. 2 (1982) 86.

[17] A. Henglein, Ber. Bunsenges. Phys. Chem. 86 (1982) 301.

[18] B.R. Eggins, J.T.S. Irvine, E.P. Murphy, J. Grimshaw, J. Chem. Soc., Chem. Commun. (1988) 1123.

[19] B.R. Eggins, J.T.S. Irvine, J. Grimshaw, Solar Energy 45 (1990) 27.

[20] B.R. Eggins, P.K.J. Robertson, J.H. Stewart, E. Woods, J. Chem. Soc., Chem. Commun. (1993) 349.

[21] P.K.J. Robertson, B.R. Eggins, J. Chem. Soc., Perkin Trans. 2 (1994) 1829.

[22] A.H.A. Tinnemans, T.P.M. Koster, D.H.M.W. Thewissen, A. Mackor, Nouv. J. Chem. 6 (1982) 373.

[23] T. Rajh, O.J. Mici, Bull. Soc. Chem. Beograd 8 (1982) 335.

[24] J.G. Calvert, J.N. Pitts, Photochemistry, Wiley, New York, 1973.

[25] N.S.T. Lui, O.A. Roels, Anal. Biochem. 8 (1970) 202.

[26] E.A. McMullan, Ph.D. Thesis (CNAA), Ulster Polytechnic, 1985.

[27] A. Hagfeldt, M. Grätzel, Chem. Rev. 95 (1995) 49.

[28] M.R. Hoffmann, S.T. Martin, W. Choi, D.W. Bahnemann, Chem. Rev. 95 (1995) 69.

[29] M. Kanemoto, T. Shiragami, C. Pac, S. Yanagida, J. Phys. Chem. 96 (1992) 3521.

[30] J. Hawecker, J. Lehn, R. Zeissel, Helv. Chim. Acta 69 (1986) 1990.

[31] A.S. Feinar, A.J. McEvoy, N. Vlachopoulos, M. Grätzel, Ber. Bunsenges. Phys. Chem. 91 (1987) 399.

[32] N.S. Lewis, G.A. Lewis, see reference 7, p. 263.

[33] E.R. Carraway, A.J. Hoffmann, M.R. Hoffmann, Environ. Sci. Technol. 28 (1994) 786.

[34] A. Mills, S. Le Hunte, J. Photochem, Photobiol. A, 108, 1997, 1, and references therein.

[35] B.R. Eggins, J. Chem. Soc., Chem. Commun. (1969) 1267.

[36] C. Amatore, J.-M. Saveant, J. Am. Chem. Soc. 103 (1981) 5021.

[37] J.T.S. Irvine, D. Phil. Thesis, University of Ulster, 1986.

[38] M. Kanemoto, K. Ishihara, Y. Wada, T. Sakata, H. Mori, S. Yanagida, Chem. Lett. (192) 835.

[39] J.R. White, A.J. Bard, J. Phys Chem. 89 (1985) 1947.

[40] H. Gerischer, J. Electroanal. Chem. 58 (1975) 263.

[41] A. Henglein, Pure Appl. Chem. 56 (1984) 1215.